Toxicology Reports 8 (2021) 1143–1155

Contents lists available at ScienceDirect

Toxicology Reports

journal homepage: www.elsevier.com/locate/toxrep

Exploitation of traditional healing properties, using the nanotechnology's advantages: The case of curcumin

Angeliki Liakopoulou [a], Elena Mourelatou [b], Sophia Hatziantoniou [a,*]

[a] Laboratory of Pharmaceutical Technology, Department of Pharmacy, School of Health Sciences, University of Patras, 26504, Patras, Greece
[b] Laboratory of Pharmaceutical Technology, Department of Life and Health Sciences, School of Sciences and Engineering, University of Nicosia, 46 Makedonitissas Avenue, CY-2417, P.O. Box 24005, CY-1700, Nicosia, Cyprus

ARTICLE INFO

Handling Editor: Dr. A.M. Tsatsakis

Keywords:
Solid lipid nanoparticle
Nanostructured lipid carrier
Nanoemulsion
Curcumin
Topical application
Occlusion
Wound healing

ABSTRACT

Curcumin (CUR) has a long history of use as an antimicrobial, anti-inflammatory and wound healing agent, for the treatment of various skin conditions. Encapsulation in nanocarriers may overcome the administration limitations of CUR, such as lipophilicity and photodegradation. Lipid nanocarriers with different matrix fluidity (Solid Lipid Nanoparticles; SLN, Nanostructured Lipid Carriers; NLC, and Nanoemulsion; NE) were prepared for the topical delivery of curcumin (CUR). The occlusive properties and film forming capacity, as well as the release profile of incorporated CUR, its protection against photodegradation and wound healing were studied *in vitro*, using empty nanocarriers or free CUR as control. The results suggest that incorporation of CUR in nanocarriers offers a significant protection against photodegradation that is not influenced by the matrix fluidity. However, this characteristic regulates properties such as the occlusion, the release rate and wound healing ability of CUR. Nanoparticles of low fluidity provided better surface occlusion, film forming capacity and retention of the incorporated CUR. All nanocarriers but especially NLC, achieved faster wound healing at lower dose of incorporated CUR. In conclusion, nanotechnology may enhance the action of CUR against skin conditions. Important characteristics of the nanocarrier such as matrix fluidity should be taken into consideration in the design of CUR nanosystems of optimal efficiency.

1. Introduction

Since ancient times, nature was the only place where people could explore to cover their daily nutritional or therapeutic needs. Nowadays the medicinal benefits of different natural products are a scientific area of great research interest [1]. Many plant origin ingredients have been used in herbal formulations due to their promising properties as antioxidants or for their anti-ageing, anti-inflammatory, antimicrobial and moisturizing effect. The efficient topical delivery of these ingredients is crucial to their action and has been studied extensively during the last decades. Several natural products such as vitamins (e.g vitamin C, vitamin E, vitamin A), essential oils (e.g. rosemary – *Rosemarinus officinalis* L., tea tree – *Melaleuca alternifolia*), non-essential oils (e.g. jojoba oil – *Simondsia chinensis*, coffee – *Coffea arabica* L.) and polyphenols (e.g. quercetin from *Sophora japonica* L., resveratrol from *Arachis hypogaea* Linn, Vaccinium spp., curcumin from *Curcuma Longa*) have been incorporated in various delivery systems in order to improve their solubility, stability, bioavailability, skin permeation or to reduce limitations such as cytotoxicity or volatility [2]. A characteristic example of a plant that is widely used and its ingredients are extensively studied is *Curcuma longa* (Linn.) that belongs to the ginger family or Zingiberaceae [3]. The rhizomes of this plant provide a spice known as Turmeric that is also characterized as the "Golden Spice", the "Indian Saffron" or the "Herb of the Sun" because of its orange-yellow color [4,5]. Centuries of use as flavoring agent, beauty product, dye, and for medicinal purposes have established its safety and benefits [6,4]. Its first appearance was

Abbreviations: CUR, curcumin; SLN, solid lipid nanoparticles; NLC, nanostructured lipid carriers; NE, nanoemulsion; TG, triglyceride; WFI, water for injection; RT, room temperature; EtOH, ethanol; MeOH, methanol; PBS, phosphate buffered saline; DMEM, Dulbecco's modified eagle medium; DPBS, Dulbecco's phosphate buffered saline; BSA, bovine serum albumin; P/S, penicillin/streptomycin; FBS, fetal bovine serum; DMSO, dimethyl sulfoxide; CA, cellulose acetate; RH, relative humidity; SEM, scanning electron microscopy; UV-VIS, ultraviolet – visible spectrophotometry; SD, standard deviation; PdI, polydispersity index; DLS, Dynamic Light Scattering; ELS, Electrophoretic Light Scattering.

* Corresponding author.
E-mail addresses: aliakop@upatras.gr (A. Liakopoulou), mourelatou.e@unic.ac.cy (E. Mourelatou), sohatzi@upatras.gr (S. Hatziantoniou).

https://doi.org/10.1016/j.toxrep.2021.05.012
Received 14 February 2021; Received in revised form 2 April 2021; Accepted 26 May 2021
Available online 28 May 2021
2214-7500/© 2021 The Author(s). Published by Elsevier B.V. This is an open access article under the CC BY-NC-ND license (http://creativecommons.org/licenses/by-nc-nd/4.0/).

probably recorded in China by 700 AD and its fame traveled west reaching East Africa by 800 AD, West Africa by 1200 AD, and Jamaica in the 18th century. In 1280, during a travel to China, Marco Polo in his notes compared turmeric with saffron [7,8]. From its first use until today turmeric has a symbolic usage which relates to Hindu ceremonies such as weddings [9]. The history of turmeric dates many years ago, when it has been used in traditional Indian and Chinese medicine for the treatment of various diseases, mainly connected with inflammatory conditions or bacterial infections [10,11]. Especially in Ayurvedic therapy turmeric was used for the relief of digestive disorders and for wounds cleansing [11,5]. In 250 AD turmeric has been referred as ingredient of an ointment against symptoms of food poisoning [7,8]. In China, it was traditionally used for urticaria, inflammatory conditions of joints, and skin allergies [7]. It can be administered orally, topically, or via inhalation for the treatment of many skin conditions, injuries, infections, stress, and depression [12,6]. India keeps the main production of Turmeric, but it is also grown in tropical parts of America, Africa and Pacific Ocean Islands [11,5,9]. The composition of this herb includes different substances such as phenols, terpenoids and other groups of molecules such as curcuminoids: Curcumin (CUR), Demethoxycurcumin and Bisdemethoxycurcumin [12,13]. The presence of CUR in the herb is responsible for the characteristic color of its rhizome [4]. The discovery of CUR dates two centuries ago. A pure preparation of CUR was obtained by Vogel Jr. in 1842, but this attempt was never published. The chemical structure of CUR as diferuloylmethane, or 1,6-heptadiene-3,5- dione-1, 7-bis (4-hydroxy-3-methoxyphenyl)-(1E, 6E) was first identified by the team of Milobedzka and Lampe in 1910, but was published in 1913. Later, Srinivasan separated and quantified the curcuminoids in *Curcuma longa* by chromatography. In 1937 the first study using CUR for human diseases was published, while in 1949 the antibacterial effect of CUR was documented [7,14]. Due to its polyphenolic nature, CUR possesses a multitargeting ability that is linking it to various pharmacological actions such as anti-cancer, anti-arthritic, antimicrobial, anti-inflammatory, antioxidant, anti-diabetic and wound healing [7,15]. According to Hashemzaei and coworkers a combination of resveratrol, CUR, and gallic acid inhibited reactive oxygen species formation, lipid peroxidation and attenuated Glyoxal-induced renal cytotoxicity [16]. Moreover, CUR has received much attention in several neurodegenerative diseases, such as Alzheimer's. Interestingly, the consumption of high doses of CUR in India might be responsible for the significant lower prevalence of dementia compared to US [15]. In addition, Stancioiu and coworkers recommend the use of CUR for treatment of signs of porphyria, asthma or for alleviating inflammation and pain [17]. However, CUR has several physicochemical characteristics that render its formulation and clinical applications difficult [4]. First of all, CUR is an hydrophobic, photosensitive molecule that is stable in acidic or neutral environment, while under alkaline conditions it is easily degraded and changes its color from yellow-orange to red [4,9]. It is also characterized by low oral bioavailability, high metabolic rate and low levels in plasma and tissue [4,9,7,1]. On the other hand, topical route is an alternative to the oral delivery of CUR with numerus benefits [4]. According to the literature, a few human clinical trials have been conducted applying CUR formulations, both orally (tablets) and topically (creams, gels, herbal oils), for the treatment of various skin diseases such as acne, eczema, facial photoaging, pruritus, psoriasis, radiation-induced dermatitis and vitiligo [18,6]. Currently 246 clinical trials are documented (of which 115 completed) using turmeric ingredients, including CUR, as therapeutic or dietary supplement against a wide variety of conditions such as cancer, periodontitis, rheumatoid arthritis, type 2 diabetes and depression, as well as cardiovascular, gynecological, Crohn's, Alzheimer's and chronic kidney diseases, among others [15,59]. Specifically, 12 of those clinical trials concern the action of orally or topically administered CUR formulations against various skin disorders. Oral application of CUR or turmeric has been undergone clinical trials for the treatment of several skin conditions such as radiation dermatitis, UV-induced skin erythema, mycosis fungoides or Sézary syndrome, sebum production, chronic psoriasis vulgaris. A limited number of clinical trials on topical application have been conducted such as topical application of turmeric extract for the treatment of psoriasis, acetyl zingerone for cosmetic purposes and CUR against HIV-infection or radiation dermatitis. However, some limitations of these studies have set the need for more investigation. Nanotechnology may contribute in overcoming the limitations posed by conventional therapeutic approaches with CUR, such as the poor bioavailability and molecule stability, thus attracting a lot of research interest. Due to the nature of the molecule the ability to penetrate into cells is limited, but Guo and coworkers proved that nanocarriers enhance the ability of CUR to enter cells, a process known as endocytosis [19]. The encapsulation of CUR into nano vehicles is an alternative option that provides improved water solubility, skin penetration, controlled release, reduced dose, low toxicity among others [1,4,12]. According to the literature, CUR has been incorporated into several novel formulations including nanoemulsions (NE), solid lipid nanoparticles (SLN), nanostructured lipid carriers (NLC), micelles, silica nanoparticles, silver nanoparticles, liquid crystal nanoparticles, polymeric nanoparticles, cyclodextrins, liposomes, niosomes, ethosomes, transferosomes, nanospheres, nanocapsules and phospholipids complexes. All these systems have been studied for cutaneous delivery of CUR in order to target affected tissues for the treatment of skin conditions like inflammation, acne, psoriasis, photoaging, wounds, melanoma, cutaneous leishmaniasis and infections related to bacteria, fungi or viruses [4,10,12,13,20,21]. Parameters such as the method of preparation and fluidity of the lipidic carrier seems to be of importance as they regulate properties such as nanocarrier size distribution, endocytosis, and pharmacological response [15,22]. Moreover, a lot of research has been conducted both in vitro on cell lines and in vivo on animal models, but less on healthy people or even patients, to evaluate the safety of CUR administration. According to these studies CUR has been characterized as safe for human use even at high doses with no severe side effects [7,20,23].

In the present study, three lipid nanocarriers with different matrix fluidity (i.e., SLN, NLC, NE) were prepared for CUR encapsulation. Their ability to be used as topically applied dosage forms, for the relief of symptoms of various skin diseases, such as psoriasis, acne and seborrheic dermatitis, was assessed. Specifically, the aim of this work was to evaluate the impact of the nanocarrier characteristics such as the matrix fluidity, on the regulation of properties like the film forming capacity, occlusive index, and wound healing that play a significant role in the treatment of skin conditions. Moreover, the release profile of CUR from the nanocarriers, and their ability to protect CUR from sunlight exposure were studied, to evaluate the full potential of these dosage forms. A comparison between these three different nanocarriers may indicate the optimal system for topical delivery of CUR. While previous studies have shown that the size of nanocarriers is an important factor that influences their efficiency [24,25], our results suggest that CUR action and properties that are important in the treatment of skin conditions, could be further enhanced, taken into consideration the matrix fluidity.

2. Materials and methods

2.1. Materials

2.1.1. Chemicals

The chemicals were of pharmaceutical, cosmetic, or analytic grade. Curcumin (Acros Organics, New Jersey, USA), saboderm TCC (SABO S.p.A., Bergamo, Italy), softisan 100 (Sasol GmbH, Hamburg, Germany), solutol HS 15 (BASF, Ludwigshafen, Germany), emulmetik 900 (Lucas Meyer Cosmetics, Champlan, France), water for injection (WFI) (Demo S.A., Pharmaceutical Industry, Kryoneri, Attica, Greece), ethanol (absolute, purity ≥99.8 %) (Acros Organics, New Jersey, USA), methanol (purity ≥99.8 %) (Honeywell Riedel-de Haën, Seelze, Germany), phosphate buffered saline (PBS) (Sigma Aldrich, Darmstadt, Germany), L-ascorbic acid (Sigma Aldrich, Darmstadt, Germany) and citric acid

(Chemco, Pharmaceutical Industry, Ilion, Attica, Greece) were purchased.

2.1.2. Cell culture reagents

Dulbecco's modified eagle medium (DMEM) (Pan-biotech, Aidenbach, Germany), Dulbecco's phosphate buffered saline (DPBS) (Pan-biotech, Aidenbach, Germany), bovine serum albumin (BSA) (Pan-biotech, Aidenbach, Germany), trypsin/EDTA in Hank's balanced salt solution (HBSS) (Biosera, Nuaille, France), penicillin/streptomycin (P/S) (Biosera, Nuaille, France), fetal bovine serum (FBS) (PanReac AppliChem, Darmstadt, Germany), and dimethyl sulfoxide (DMSO, purity 99.5 %) (PanReac AppliChem, Darmstadt, Germany) were also purchased. Mouse embryonic fibroblasts (NIH3T3) were donated by Laboratory of Molecular Pharmacology, University of Patras, Rio, Greece.

2.2. Methods

2.2.1. Preparation of nanocarriers

Three types of CUR loaded nanocarriers were prepared namely CUR-SLN, CUR-NLC and CUR-NE. Additionally a corresponding set of empty nanocarriers (SLN, NLC, NE) was also prepared for comparison. The difference between each carrier is the viscosity of their internal phase that is regulated by the physical state of the triglyceride (TG) it contains. Table 1 summarizes the formulations, their composition (% w/w) and the lipid phase ratio applied for the investigations presented.

The preparation of nanocarriers was performed by hot emulsification method followed by probe sonication, as described by Rapalli et al. [26] with minor modifications. Firstly, a conventional emulsion was formed by heating (65−70 °C) separately the aqueous and lipid phase and then adding dropwise the aqueous phase to the lipid phase, under stirring (200−300 rpm) on a Heating Magnetic Stirrer (Velp Scientifica, Usmate Velate (MB), Italy). CUR was accurately weighted (Mettler digital lab scale balance analytical AE166 Delta Range, max: 166 g, accuracy: 0.0001 g, Mettler Instrument Corp., Hightstown, New Jersey, USA) to obtain 0.05 % w/w final concentration, and it was added to the molten lipid phase before the emulsification process. The emulsion was cooled under stirring (500 rpm, 30 min) till room temperature (RT). The prepared emulsion was further homogenized by ultrasonication (Vibra cell™, Sonics & Materials, Newtown CT, USA, with amplitude 83 %) for 1 min/mL to form CUR-loaded SLN, NLC and NE. The CUR-loaded nano dispersions were cooled down by vortexing (8000 rpm, Vortex-Genie 2, Scientific Industries, Bohemia, New York, USA) till RT and then stored at 4 °C in light-protected sealed containers.

2.2.2. In vitro occlusion test

The occlusive properties of CUR-loaded and empty nanocarriers were determined using a modified in vitro occlusion test [27]. Beakers (capacity: 50 mL, internal diameter: 51 mm) were filled with tap water (40 mL), covered with cellulose substrate (CA Membrane Filter, 47 mm, 0.45 um, Filter-Bio, Nantong, China), and sealed perimetrically with sealing film leaving the top surface free. 500 µl of each sample with 3% w/v lipid content (corresponding to 0.7 mg/cm^2) was spread on the cellulose substrate. Each sample (S) was tested in triplicate while three beakers were left without applying any sample and used as reference (R). The beakers were stored at 32 ± 0.5 °C and 50–55 % of relative humidity (RH) for 48 h. The weight of each beaker was monitored immediately after sample application and at 6, 24, and 48 h of incubation. For the calculation of the occlusion factor F the (Eq. (1)) was used:

$$F = \left(\frac{R - S}{R}\right) x100 \quad (1)$$

where, R and S are the weight difference of each beaker from the initial measurement representing water loss of the reference and sample respectively. According to Shrotriya et al. [28] in a scale of 100 an index of 0 shows no effect. F = 10 was set as the minimum accepted score.

Table 1
Composition of all investigated formulations in % (w/w) and lipid phase ratio.

MATERIALS	INCI NAME	FUNCTION	NANOCARRIERS		
			SLN	NLC	NE
			Composition (% w/w)		
Saboderm TCC	Caprylic / Capric Triglyceride mix	Liquid TG	0	0.5	1.5
Softisan 100	Hydrogenated Coco-glycerides	Solid TG	1.5	1	0
Emulmetik 900	Lecithin	Emulsifier	1.5	1.5	1.5
Solutol HS 15	Macrogol (15)-hydroxystearate	Non-ionic solubilizer & co-emulsifier	0.05		
CUR	Turmeric (Curcuma Longa dry extract)	Biomolecule	0.05		
WFI	Aqua	Continuous phase	96.9		

2.2.2.1. Scanning Electron Microscopy (SEM).

The film forming capacity of the samples was monitored by scanning electron microscopy (SEM). Cellulose substrates after the occlusion test were sputter-coated with carbon in JEOL JEE-4B carbon – coater. Then, the samples were examined in a scanning electron microscope (JSM5600LV, JEOL, Japan), operating at an accelerating voltage of 25 kV. The chemical composition of the samples was analyzed based on EDS spectra of an Oxford Instruments X-ray Energy Dispersive Spectrometer. The images of the cellulose substrate without any sample were used as reference [27,29].

2.2.3. In vitro release kinetics study

In order to investigate the release behavior of CUR from nanocarriers the dialysis method described by Kumar et al. was used with minor modifications [30]. Dialysis of each sample was carried out through dialysis bag with high retention capacity (99.99 %) and a molecular mass cut off 12.4 kDa, (dialysis tubing, Sigma Aldrich, Darmstadt, Germany). A mixture of PBS/EtOH (1:1, v/v) and 0.1 % L-ascorbic acid was used as the dissolution medium (pH = 5.5, citric acid 0.1 M). Before using them, the dialysis bags were soaked under continuous water flow for 30 min and then for 15 min under heated (50 °C) distilled water. An aliquot of 1.0 mL (equivalent to 0.5 mg CUR) freshly prepared CUR-SLN; CUR-NLC or CUR-NE dispersion was transferred into the dialysis bag and placed in a beaker containing 200 mL of dissolution medium. The beakers were placed in a shaking water bath and maintained at 32 ± 0.5 °C throughout the experiment. Aliquots of 3 mL of the dissolution medium were withdrawn at the predefined time points (10, 30, 60, 120, 180, 240, 480, 720, 1440, and 1920 min) and replaced by fresh medium. CUR concentration was determined by spectrophotometry, measuring UV absorbance at 425 nm (UV-1800, UV–vis Spectrophotometer, Shimadzu, Duisburg, Germany), and finally the percentage of released CUR was calculated against calibration curves. The experiment was performed in triplicate for all formulations tested. To study the release mechanism of CUR from prepared lipid nanocarriers, data obtained from *in vitro* release studies were fitted to various mathematical models [31] such as zero order, first order, Higuchi, Hixson-Crowell, Korsmeyer-Peppas, and Kopcha release kinetic equations (Table 2). The plotted experimental data were fitted using the linear regression fitting option of the Microsoft Excel and the regression coefficient (R^2) was obtained for each graphical presentation. The value of the coefficient determines the most suitable mathematical model that describes drug release kinetics [32–35].

2.2.4. Photo-degradation studies

The photostability of the three CUR-loaded nanocarriers (CUR-SLN; CUR-NLC; CUR-NE) was tested by photo-degradation studies. A hydro-alcoholic solution (MeOH:WFI, 2:8 v/v) of free CUR (0.5 mg/mL) was used as control. All samples were sealed in 10 mL transparent vials and exposed to direct sunlight for a period of 22 days. The colloidal stability

Table 2
Mathematical models used for the description of release kinetics.

Model	Equation	Plot
Zero Order Model	$Q_0 - Q_t = K_0 t$, (i), (ii), (iv)	cumulative % of CUR released vs. time
First Order Model	$LogQ_t = LogQ_0 - K_1 t/2.303$, (i), (ii), (iv)	Log cumulative % of CUR remaining vs. time
Higuchi Model	$Q_t = K_H t^{1/2}$, (ii), (iv)	cumulative % of CUR released vs. square root of time
Hixson-Crowell Model	$(Q_0^{1/3} - Q_t^{1/3}) = K_{HC}t$, (i), (ii), (iv)	cube root of % CUR remaining vs. time
Korsmeyer-Peppas Model	$M_t/M_\infty = K_{KP}t^n \rightarrow Log\ (M_t/M_\infty) = logK_{KP} + nLogt$, (iii), (iv), (v)	Log cumulative % CUR released vs. Log time
Kopcha Model	$Q_t = At^{1/2} + Bt$, (ii), (vi), (vii)	cumulative % of CUR released/time vs. 1/square root of time

(i) Q_0 : the initial amount of CUR in nanoparticles, (ii) Q_t : the amount of CUR released at time *t*, (iii) M_t/M_∞ : the fraction of CUR released at time *t*, (iv) K_0, K_1, K_H, K_{HC}, K_{KP}: the model kinetic constant, (v) *n*: the diffusion exponent, (vi) *A*: the diffusion rate constant, (vii) *B*: the erosion rate constant.

of the samples was assessed by exposing the dispersions to direct sunlight and measuring their size distribution, polydispersity index (PdI), ζ-potential and CUR content before irradiation and at predetermined time intervals for a period of 22 days. The average hydrodynamic diameter (mean size), PdI, and ζ-potential of all samples were monitored by Dynamic or Electrophoretic Light Scattering (DLS or ELS), respectively (Malvern Instruments Ltd., Malvern, UK) after their dispersion in WFI. The CUR content (mg/mL) of the samples was determined using UV–vis Spectroscopy (UV-1800, UV–vis Spectrophotometer, Shimadzu, Duisburg, Germany) [36–38].

2.2.5. Wound healing – scratch assay

2.2.5.1. Cell culture. Normal skin fibroblasts (designated NIH3T3) were cultivated in monolayers using flasks (Nunc EasYFlask, 75 cm^2, Fisher Scientific, Leicester, UK), and were incubated under usual culturing conditions of 37° C, 95 % RH and 5% CO_2. The culture medium consisted of DMEM, 10 % FBS and antibiotics (P/S). When cultures were 80–90 % confluent, the cells were detached from the flask bottom after treatment with 0.25 % trypsin/EDTA in HBSS solution for 3−5 min. Then, trypsin was deactivated by fresh medium addition. Confluent cell cultures were passaged by splitting process three times per week [39].

2.2.5.2. Scratch assay. After trypsinization, 3×10^5 cells/well were seeded in 24-well plates (Nunc EasYFlask, 75 cm^2, Fisher Scientific, Leicester, UK) to grow in a monolayer for 48 h. Before the scratch creation, cells were submitted to a starvation process for 2−3 hours under normal culturing conditions of 37 °C, 95 % RH and 5% CO_2. The starvation medium consisted of DMEM supplemented only with antibiotics (P/S). Then a sterile plastic cell scratcher with 1 mm width (SPLScar Scratcher, SPL Life Sciences Co., Korea) was held vertically to scratch across in each well. The detached cells were removed by washing with 500 μL DPBS. 1.0 mL of fresh medium with or without diluted samples of CUR was added afterwards and incubated for 48 h. Samples containing CUR in different dilutions (0.10, 0.30, 1.0, 3.0, 9.0, 30.0 μM) were examined: (a) CUR dissolved in DMSO (DMSO concentration did not exceed 1.0 % in each well), (b) CUR encapsulated in different lipid carriers (CUR-SLN; CUR-NLC; CUR-NE) and (c) empty nanocarriers (SLN; NLC; NE). Fresh medium with 2% FBS was used as positive control, while negative control was supplemented with 0.1 % BSA, instead of 2% FBS. Negative control was also used as diluent. The scratch closure was monitored at predefined time points (0 h, 24 h and 48 h) using a micro-camera (Soft Plus, Callegari, Parma, Italy) at 400x magnification and 640 × 480 resolution [39]. The percentage of wound closure was determined at predefined time points according to (Eq. (2)):

$$(\%)\text{Wound Closure} = \left(\frac{A_{t0} - A_{\Delta t}}{A_{t0}}\right) x\ 100\% \quad (2)$$

Where, A_{t0} is the initial wound area (Length x Width, t = 0), $A\Delta_t$ is the wound area after n hours of the initial scratch (Length x Width, t=Δt), both in mm^2 [40].

2.3. Statistical analysis

The results are reported as mean values ± standard deviation (SD) of measurements executed in triplicate. The statistical significance of differences was determined using Student's *t*-test (Microsoft Office 365 Excel 2016, Redmond, WA, USA) and two-way ANOVA in Minitab 19 Statistical Software (Minitab Ltd., Software Company, Coventry, UK) followed by Tukey's post-hoc test for multiple comparisons. Statistical significance was accepted for $p < 0.05$.

3. Results

3.1. Occlusion efficacy

3.1.1. In vitro occlusion test

The occlusion index (F) was calculated for each nanocarrier after 6, 24, and 48 h of application of the formulation, setting F = 10 as the minimum accepted score (Fig. 1). None of the empty-nanocarriers scored F > 10, at 6 h, while at 24 h only SLN achieved the highest score ($F = 30.95 \pm 5.63$, $p < 0.05$) and continued to grow at higher levels ($F = 36.18 \pm 6.01$, $p < 0.005$ at least up to 48 h (Fig. 1.a). CUR-SLN achieved high scores ($F = 29.88 \pm 10.74$, $p < 0.05$) at 6 h that at 24 and 48 h were maintained at similar levels ($p > 0.05$) with SLN ($F = 31.04 \pm 7.34$ and $F = 31.78 \pm 7.90$, respectively) (Fig. 1.a). The F calculated for NLC and NE did not achieve scores above 10 at any time point indicating pour occlusive properties of the films. CUR-NLC did not differ significantly from NLC, while F for CUR-NE was significantly enhanced at every time point ($p < 0.05$) compared to NE but not significantly above F = 10 (Fig. 1.b,c).

3.1.2. Scanning Electron Microscopy (SEM)

The morphology of the films formed by each sample on cellulose substrate was assessed as per their integrity (appearance of holes) and their thickness (ability to hide the cellulose fibers) (Fig. 2). Films formed by both SLN and NLC appeared more intact and thicker in comparison to the ones formed by NE that seems to form less compact and more thin film. The incorporation of CUR ameliorates the quality of the film formed by each sample that appear more continuous and thicker.

3.2. In vitro release study

in vitro drug release study was performed for CUR-loaded nanocarriers. The (%) cumulative CUR release was monitored at predetermined time points. The release profile of each nanocarrier is illustrated in Fig. 3. A burst biphasic profile [41] was observed for all CUR-loaded nanocarriers. Initially a rapid release of CUR was manifested for the first 240 min, followed by sustained release until the end of the study (1920 min). Higher burst release was observed for CUR-NE, reaching 55.89 ± 1.94 % ($p < 0.001$), while only 31.32 ± 3.36 % for CUR-SLN and 37.14 ± 4.39 % for CUR-NLC was released at the same time point. At the end of the study (1920 min) the NE nanocarrier had released a 66.60 ± 3.82 % of CUR ($p < 0.001$), while at the same time point a 35.19 ± 1.60 % and 44.79 ± 4.16 % of CUR was released by SLN and NLC nanocarriers respectively.

3.2.1. Release kinetics

By fitting all models to release data, correlation coefficients (R^2), release rate constants (A, B, K) and release exponent (n) values were

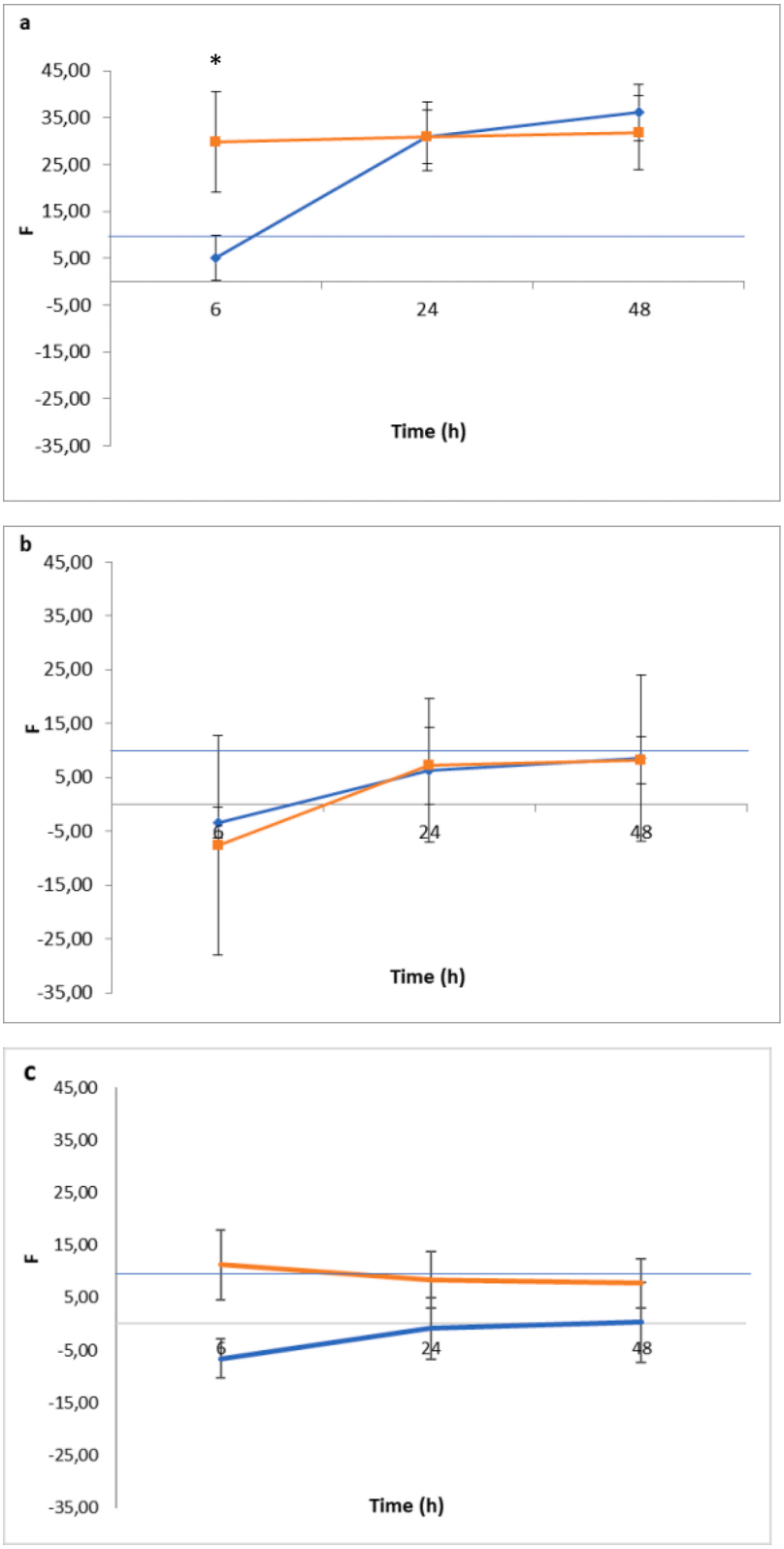

Fig. 1. Occlusive Index (F) of (–) empty and (–) CUR-loaded (a), SLN (b), NLC and (c) NE, at 6, 24 and 48 h (*: $p < 0.05$, $n = 3$). $F = 10$ was set as the minimum accepted score.

obtained for all CUR-loaded nanocarriers and the results are shown in Table 3. Release kinetics analysis revealed that CUR release did not follow zero order, first order and Hixson-Crowell kinetic models, as the plotted release data presented low linearity (R^2 values: less than 0.478, 0.333, and 0.386, respectively) for all samples.

It was also found that the *in vitro* CUR release from SLN and NLC nanocarriers was best explained by Kopcha's equation, as the plots showed the highest linearity ($R^2 = 0.977$, Fig. 4.a.(ii) & $R^2 = 0.850$, Fig. 4.b.(ii)), followed by Korsmeyer-Peppas equation ($R^2 = 0.869$, Fig. 4.a.(i)) & $R^2 = 0.856$, Fig. 4.b.(i)). While CUR release from NE was

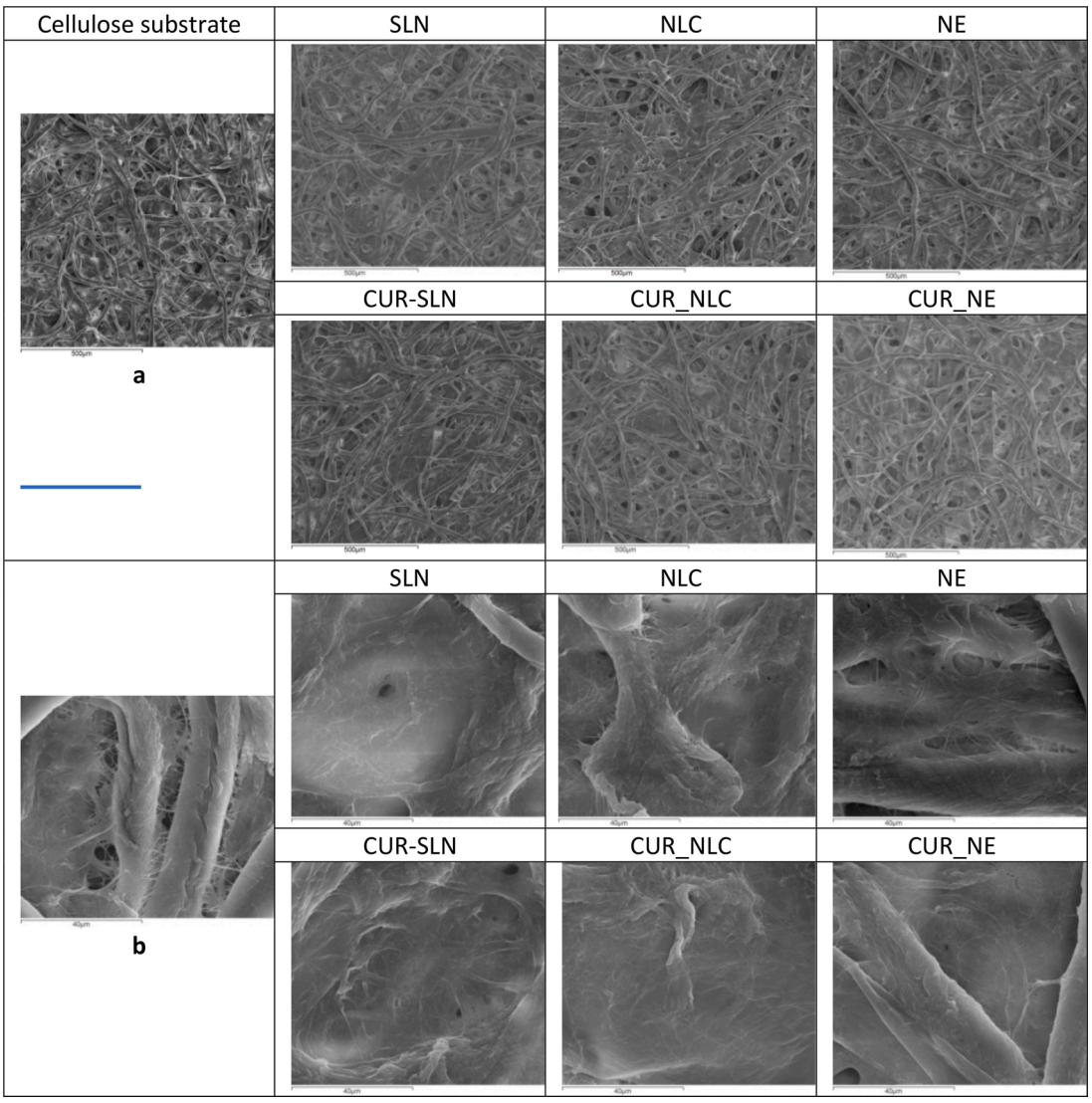

Fig. 2. SEM images of the films created from the nanocarriers on cellulose substrate, observed under × 100 (a) or × 1200 (b) magnitude. Bar represents 500 μm (a) or 40 μm (b).

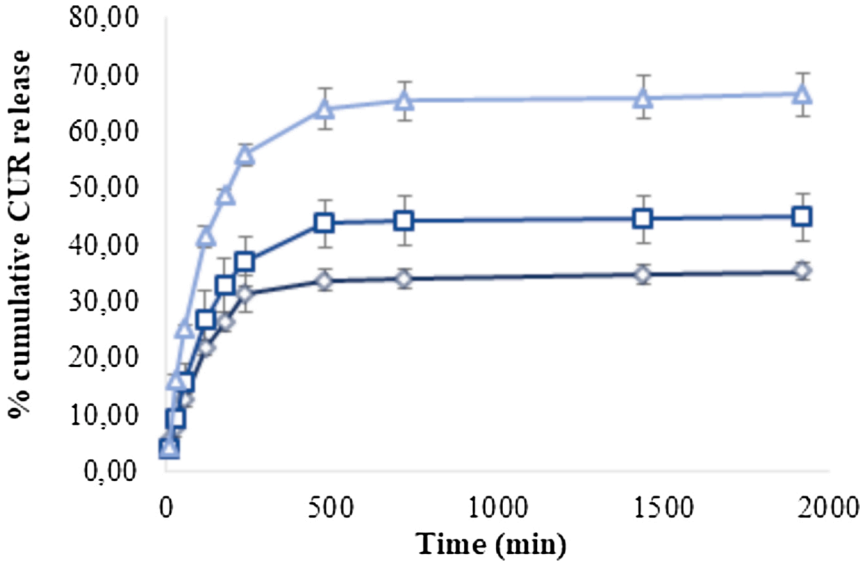

Fig. 3. *In vitro* CUR release profile from SLN (◊), NLC (□) and NE (△) nanocarriers in PBS:EtOH (1:1) + 0.1 % L-Ascorbic acid, pH = 5.5. (n = 3).

Table 3
Release kinetics parameters obtained from model fitting of the *in vitro* release data of different CUR-loaded nanocarriers.

Kinetic Model	Parameter	CUR-SLN	CUR-NLC	CUR-NE
Zero Order	R^2 (i)	0.470	0.486	0.478
	K_0 (ii)	0.012	0.017	0.024
First Order	R^2 (i)	0.364	0.335	0.299
	K_1 (ii)	0.001	0.001	0.001
Higuchi	R^2 (i)	0.688	0.708	0.699
	K_H (ii)	0.705	0.954	1.390
Hixson-Crowell	R^2 (i)	0.406	0.389	0.364
	K_{HC} (ii)	−0.001	−0.001	−0.001
Korsmeyer-Peppas	R^2 (i)	0.869	0.856	0.815
	K_{KP} (ii)	2.762	2.196	2.904
	n (iii)	0.380	0.455	0.476
Kopcha	R^2 (i)	0.977	0.850	0.616
	A (iv)	1.688	1.247	1.502
	B (v)	−0.004	0.049	0.104
	A/B	−401.88	25.40	14.47

(i) R^2: correlation coefficient, (ii) K_0, K_1, K_H, K_{HC}, K_{KP}: the model kinetic constant, (iii) *n*: the diffusion exponent, (iv) *A*: the diffusion rate constant, (v) *B*: the erosion rate constant.

fitted best to Korsmeyer-Peppas model due to higher value of regression coefficient ($R^2 = 0.815$, Fig. 4.c.(i)) compared to Kopcha's model ($R^2 = 0.616$, Fig. 4.c.(ii)). The K constant describes the rate of drug release (a high value indicates fast release [42]. The K values obtained (Table 3) indicate that CUR was released at similar rates for all lipid nanocarriers. Moreover, the value of exponent (n, indicative of the release mechanism) was found to be ranged between 0.380 for SLN to 0.476 for NE, which are responsible for (pseudo) Fickian diffusion ($n < 0.5$) [35]. On the other hand, the ratio of A/B in Kopcha model was also determined (Table 3). The Kopcha kinetics model used to determine diffusional and erosional drug release. Fickian diffusion occurs when $A/B > 1$, and if it is lower than 1, the release is controlled by erosion. In the case of being equal to 1, both diffusion and erosion are important for release mechanism [43]. The value of A/B was ranged from -401.88 for SLN, 25.40 for NLC, and 14.47 for NE. The results suggested that CUR release from the nanocarriers depend on their physical state as its release from solid SLN was mainly controlled by the erosion of the nanocarrier, while in the case of the fluid state of the NLC and NE a similar diffusion-controlled release mechanism is operated.

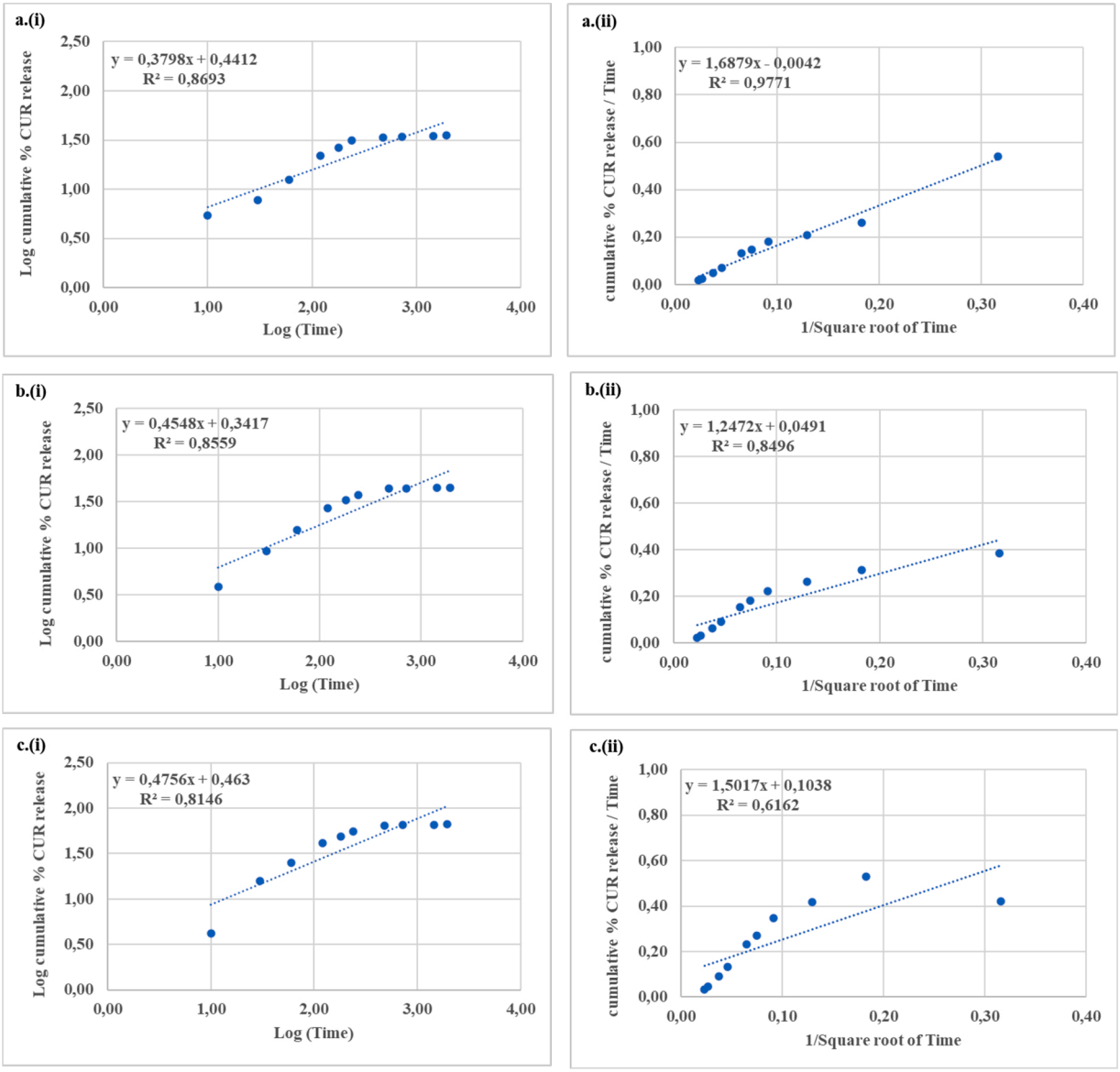

Fig. 4. Fitting of (a) CUR-SLN, (b) CUR-NLC, and (c) CUR-NE release in pH 5.5 medium by (i) Korsmeyer-Peppas, and (ii) Kopcha release kinetic model.

3.3. Photo-degradation studies

3.3.1. Size and ζ-potential

The size and ζ-potential of the three CUR-loaded nanocarriers (CUR-SLN; CUR-NLC; CUR-NE) and free CUR solution were monitored by DLS or ELS, respectively before and during radiation at predetermined time intervals. At the beginning of the process (before radiation), the size of the CUR-loaded nanocarriers ranged from 107.54 ± 3.99 nm (CUR-NE) to 119.28 ± 2.77 nm (CUR-SLN) and the PdI ranged from 0.24 ± 0.01 (CUR-NE) to 0.30 ± 0.06 (CUR-NLC) indicating good homogeneity of the dispersions. The ζ-potential was negative and its absolute value was high for all CUR-loaded nanocarriers (-66.20 ± 1.57 mV for CUR-NLC to -69.42 ± 9.09 mV for CUR-NE), indicating good colloidal stability.

The radiation process of all CUR-loaded nanocarriers left their PdI and ζ-potential unaffected ($p > 0.05$), for at least 22 days, while their mean size differed significantly ($p > 0.005$) from the initial values (Fig. 5). The mean size of CUR-NE droplets was reduced by 16.23 % ± 1.43 % at 22 days of radiation. The same reduction was noted for CUR-SLN at 15th day (14.82 % ± 0.25 %) and for CUR-NLC at 8th day (14.13 % ± 2.17 %). At 22nd day of radiation the mean size for CUR-SLN was significantly reduced by 22.73 % ± 3.05 % ($p > 0.05$) compared to CUR-NLC (19.27 % ± 3.61 %) and CUR-NE.

3.3.2. CUR stability

The CUR concentration of the CUR-loaded nanocarriers and control (CUR solution) was determined by spectrophotometry before and during radiation (Fig. 6).

After the first day of radiation, the CUR concentration of the CUR-loaded nanoparticles was reduced by 17.5 % (SLN: 18.12 % ± 8.75 %, NLC: 17.15 % ± 17.79 %, NE: 17.25 % ± 12.16 %, $p > 0.05$)) and the reduction continued in the same manner for all samples, reaching about 50 % at the 4th day and 85 % at the 8th day. The control on the other hand lost 87.68 % ± 1.34 % of the CUR content only one day of radiation (Fig. 6).

3.4. Wound healing – scratch assay

The *in vitro* wound healing capacity of empty and CUR loaded nanocarriers compared with free CUR, was assessed by the percentage of scratch area reduction (wound closure) after 24 and 48 h of incubation. The treatment with empty nanocarriers at the same lipid concentration as CUR loaded nanocarriers showed that both SLN and NE had no effect or slightly negative effect after 24 h incubation (Fig. 7.a.(i), c.(i)), while the NLC nanocarrier differed significantly, presenting a reduction of the wound area by 16.73 % ± 2.86 % ($p < 0.01$) at 3.0 μM (Fig. 7.b.(i)). After 48 h the SLN at 0.1 μM, provided a 3.43 % ± 0.81 % reduction ($p < 0.05$), while NE had no further effect. The NLC nanocarrier continued the healing activity (27.99 % ± 2.01 % at 3.0 μM, $p < 0.05$),

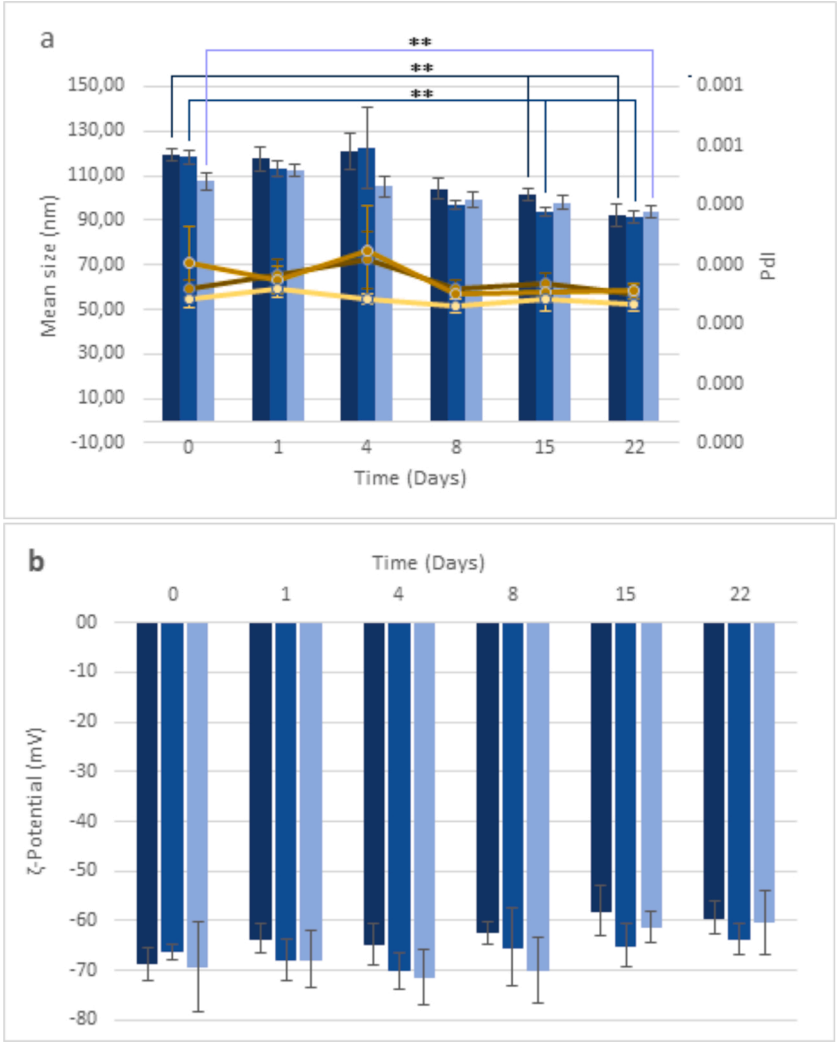

Fig. 5. Photo-degradation study monitoring (a) the mean size (■) and PdI (▪) and (b) the ζ-potential of CUR-SLN (■, ▪),CUR-NLC (■, ▪), CUR-NE (■, ▪), before (t = 0) and during radiation for a period of 22 days., (** $p > 0.005$, n = 3).

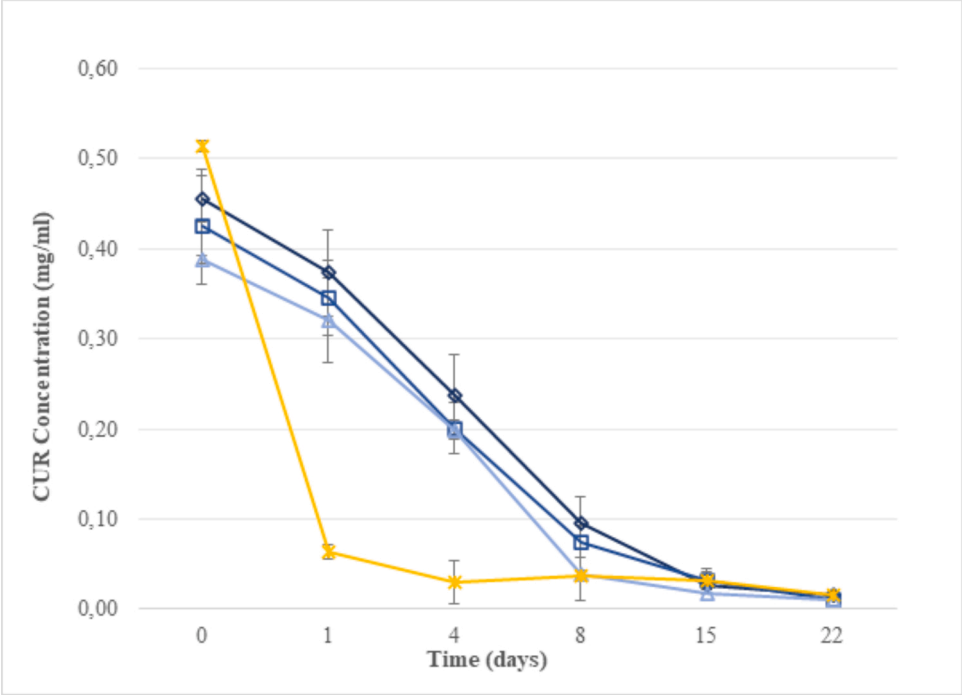

Fig. 6. Photo-degradation study of the three CUR-loaded nanocarriers CUR-SLN (◊)),CUR-NLC (□), CUR-NE(Δ)] and free CUR (x) solution monitoring the CUR content, before radiation and at predetermined time points for a period of 22 days. (n = 3).

while higher wound closure was observed at lower concentration (40.37 % ± 2.39 %, 0.3 μM, $p < 0.05$) (Fig. 8). CUR incorporation in SLN, NLC and NE seems to favor the healing effect at 24 h (4.06 % ± 0.93 %, 10.61 % ± 0.37 %, 12.29 % ± 0.75 %, respectively; $p < 0.005$) at CUR concentrations up to 9.0 μM (Fig. 7. a(ii), b(ii), c(ii) respectively). Concerning the CUR-NLC in particular, 48 h after incubation the wound healing at 0.1 μM reached up to 22.90 % ± 4.11 % ($p < 0.05$) and was similar ($p > 0.05$) to the highest free CUR healing activity observed at 1.0 μM (34.90 % ± 9,58 %, $p < 0.05$) after 48 h incubation (Fig. 7.e). At 24 h the free CUR had no effect regardless the concentration.

4. Discussion

Among other actions known so far, CUR effectively promotes wound healing at low doses either free [39] or incorporated in nanocarriers [44] as it is involving in the proliferation and migration of fibroblasts that is initiated at the second phase of wound healing. The comparison of the action of CUR free or incorporated in nanocarriers was not reported previously. To investigate the effect on wound closure of CUR incorporation in nanocarriers, a wound healing scratch assay was performed on fibroblasts (NIH3T3), because of their active participation in wound healing process [45]. Cells were treated with CUR free or incorporated in nanocarriers. Empty nanocarriers with the same lipid concentration as the CUR loaded nanocarriers were used as a control. The results of our comparative study revealed that although free CUR had a good healing action in accordance with the literature, it was clear that its incorporation in nanocarriers not only lowered significantly the dose needed but also had faster results, speeding the procedure by 50 %. While all CUR loaded nanocarriers had the same fast response, the necessary dose to achieve a wound closure comparable to the positive control (about 15 %) at 24 h varied significantly, revealing a relevance to the matrix fluidity of the nanocarrier. At this time point, a concentration of CUR-NLC 0.3 μM had the same result in wound healing as 1.0 μM for CUR-NE and 9 μM for CUR-SLN, while free CUR had no action at any concentration used. At the end of the wound healing scratch assay while CUR-NE and CUR-SLN had a slightly enhanced wound closure, CUR-NLC's action was comparable to the free CUR's reaching 35 % wound closure, with about 10 % lower dose.

The difference between nanocarriers on the performance on would healing may be attributed to their differences on the release rate of the incorporated CUR, that followed a biphasic model. The initial rapid phase (burst release) that occurs due molecules trapped near the nanocarrier surface [30] is followed by a more prolonged phase of slow release, attributed to low diffusion of the molecule through the lipidic matrix of the nanoparticles [46]. The sustained release profile of CUR loaded nanocarriers seems to be regulated by the state of lipid used on the nanoparticle matrix [47]. In accordance to these reports, our results suggested that better retention of incorporated CUR up to 60 % was achieved with nanocarriers with solid lipids (SLN) and reduced matrix fluidity (NLC), while nanocarriers with liquid lipids (NE) retained less than 40 % of CUR. Consequently, the matrix fluidity and the way of deconstruction of the nanocarrier affect the release kinetic of the encapsulated CUR. Although the early release of CUR in the high pH (7.4) environment of the scratch test assay do not favor the stability of the molecule [48] it may be useful in case of immediate control of the disease symptoms in target area, while for a prolonged treatment is necessary to maintain CUR concentration within a lower release rate [49,50].

Matrix fluidity influences the occlusion and the quality of the film that is formed on application surface. The occlusion effect is measured by the occlusion index F, which evaluates the ability of the formulation to form a lipid film on the skin [51]. The quality of this film is critical for the prevention of skin barrier, transdermal water loss and improvement of skin hydration [27,28]. According to the literature occlusion is affected by the particles' size. The particles of small size create less gaps for water evaporation and therefore the skin maintains its hydration [24, 25]. López-García & Ganem-Rondero reported that the effect of SLN and NLC dispersions present no difference and due to their size similarity, the liquid lipid of NLCs formulation has no effect on the occlusion [27].

According to our results, although all nanocarriers had a similarly small particle size, they exhibited a completely different occlusive ability. NLC and NE nanocarriers did not present a satisfactory effect. On the other hand, the higher occlusive index of more rigid nanocarriers such as SLN achieved better occlusive index, possibly attributed to the content of solely solid lipid in the formula [28], that due to the enhanced

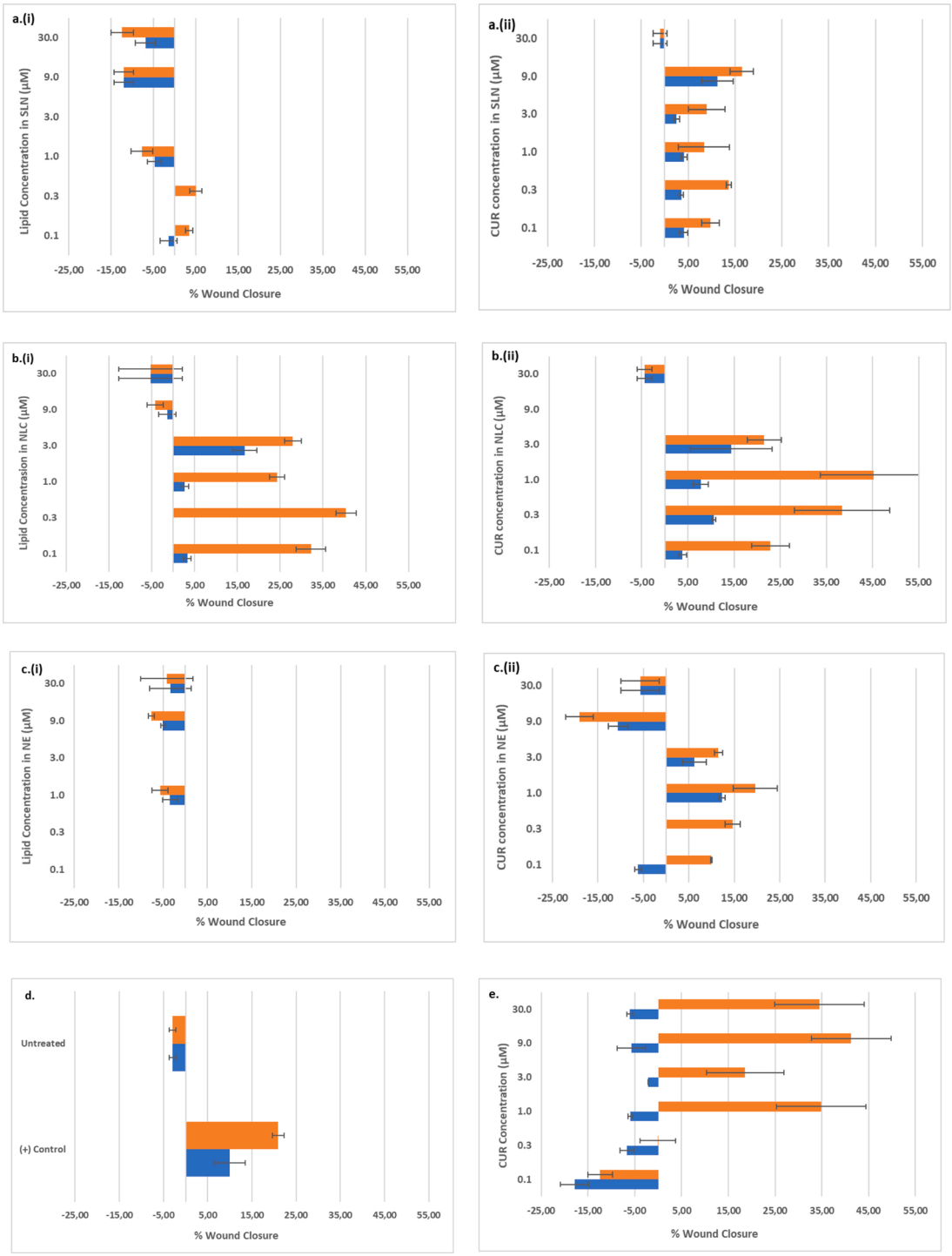

Fig. 7. Effect of (i) empty and (ii) CUR loaded (a) SLN, (b) NLC, (c) NE, (d) (+) Control / Untreated, and (e) free CUR on the wound closure at 24 (■) and 48 h (■). (n = 2).

crystallinity of the lipid matrix [52], may lead to the blocking of filter pores [53]. The faster occlusive properties that are developed after the incorporation of CUR in SLNs may be attributed to its possible influence the thermotropic properties of the lipid matrix and enhancement of the elasticity of the lipid film [54]. It appears that the formulations producing compact and thick films exhibit relatively high occlusive indexes and that CUR improves the film quality and consequently the occlusive properties of the formulation.

Finally, incorporation in all nanocarriers such as SLN, NLC or NE, seems to protect CUR against photodegradation. The protection capacity of the nanocarrier was found to be independent of the fluidity of the matrix as they were able to protect 82 % of the incorporated CUR after 24 h exposure to daylight, while only 123% of free CUR was preserved at the same time. These results are in accordance to Alkhader et al. They report that, free CUR and CUR-nanoparticles were exposed to sunlight for 6 h. The results suggested that free curcumin was immediate degraded, while the 70 % of CUR was protected from degradation in case of CUR-nanoparticles [55].

Our results demonstrate that the fluidity of the nanoparticle matrix is an important parameter that should be taken into consideration at the

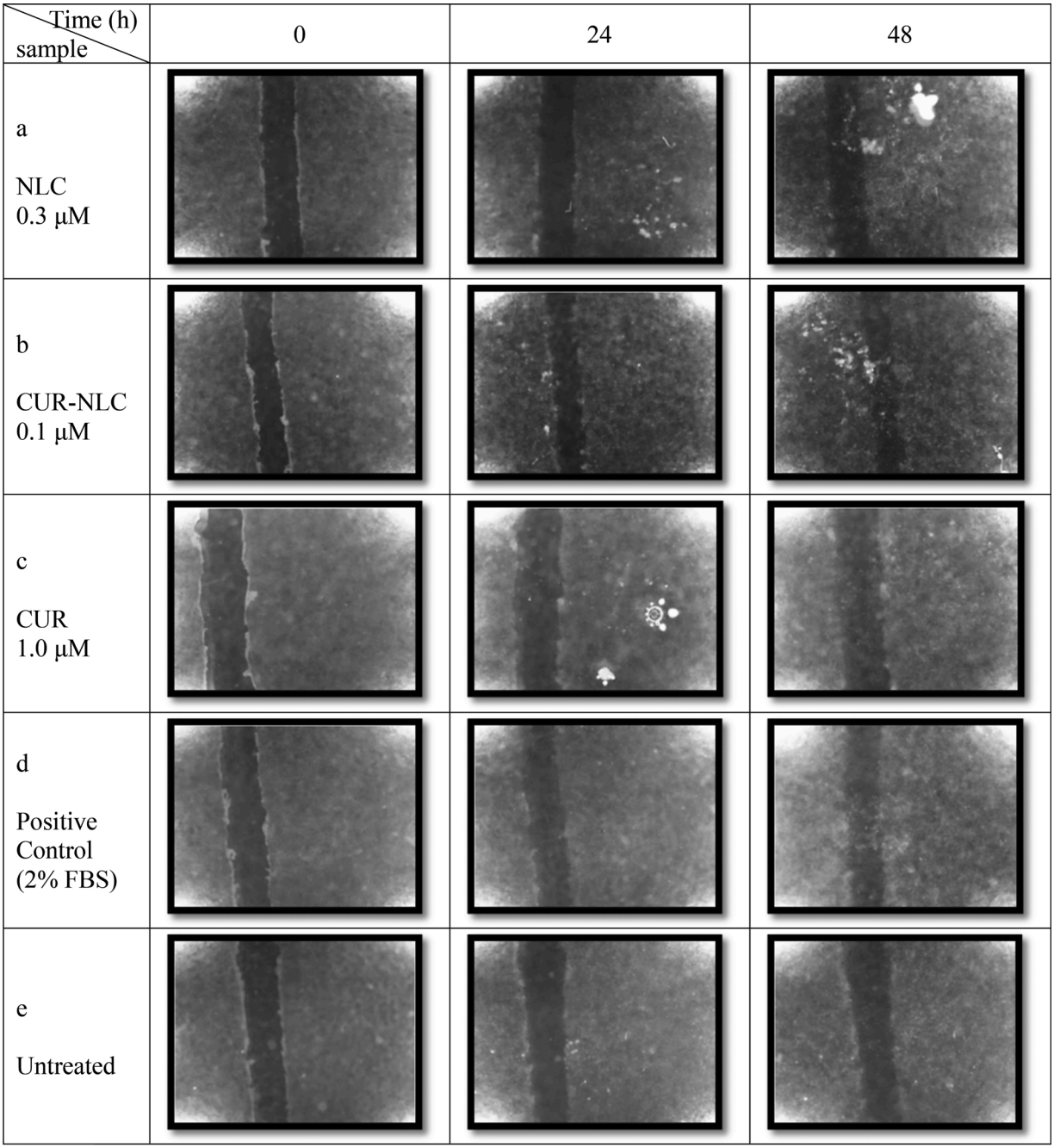

Fig. 8. Fibroblast migration after the treatment with low doses of (a), NLC (b), CUR-NLC (c), CUR (d), 2% FBS (as positive control) and (e), no treatment at 0, 24, and 48 h of incubation.

designing of CUR nanocarriers as it is influencing the wound healing action of CUR. Apart from the size of the nanocarrier, the matrix with the suitable fluidity must be chosen depending on the desirable activity. High occlusion is necessary for the treatment of skin conditions such as psoriasis [56,57], while in others such as dermatitis a low occlusion is preferable [57,58].

5. Conclusions

Nanotechnology may ameliorate the action of CUR enhancing its photostability and the pharmacological response as it can reduce the dose and time to achieve its action on wound healing. Characteristics of the nanocarrier such as the matrix fluidity must be carefully designed as it regulates the release rate of the incorporated molecule and the occlusion effect on the skin. Although the matrix fluidity seems to be irrelevant to the photoprotection that the incorporation in nanocarriers may offer to CUR, nanocarriers with low fluidity, such as SLN, may demonstrate better film forming capacity and occlusion index. Nanocarriers with medium matrix fluidity (NLC), apart from the long retention time that is similar to SLN's, may demonstrate better wound healing properties.

Funding

This research is co-financed by Greece and the European Union (European Social Fund- ESF) through the Operational Programme «Human Resources Development, Education and Lifelong Learning» in the context of the project "Strengthening Human Resources Research Potential via Doctorate Research" (MIS-5000432), implemented by the State Scholarships Foundation (IKY).

Ευρωπαϊκή Ένωση
European Social Fund

Operational Programme
Human Resources Development,
Education and Lifelong Learning
Co-financed by Greece and the European Union

ΕΣΠΑ 2014-2020
ανάπτυξη - εργασία - αλληλεγγύη

Author statement

Angeliki Liakopoulou: Investigation, Formal analysis, Writing - Original Draft, Elena Mourelatou: Investigation, Formal analysis, Writing - Review & Editing, and Sophia Hatziantoniou: Supervision, Investigation, Writing - Review & Editing.

Conflict of interest

The authors declare no conflict of interest.

Declaration of Competing Interest

The authors report no declarations of interest.

Acknowledgments

Authors would like to thank Dr. Andreas Seferlis for carrying out SEM analysis in the Laboratory of Electron Microscopy and Microanalysis, University of Patras.

References

[1] M. Gera, N. Sharma, M. Ghosh, D.L. Huynh, S.J. Lee, T. Min, T. Kwon, D.K. Jeong, Oncotarget 66680 www.impactjournals.com/oncotarget Nanoformulations of curcumin: an emerging paradigm for improved remedial application, Oncotarget 8 (39) (2017) 66680–66698. www.impactjournals.com/oncotarget/.

[2] S. Yang, L. Liu, J. Han, Y. Tang, Encapsulating plant ingredients for dermocosmetic application: an updated review of delivery systems and characterization techniques, Int. J. Cosmet. Sci. 42 (1) (2020) 16–28, https://doi.org/10.1111/ics.12592.

[3] L. Slika, D. Patra, A short review on chemical properties, stability and nano-technological advances for curcumin delivery, in: Expert Opinion on Drug Delivery, Vol. 17, Taylor & Francis, 2020, https://doi.org/10.1080/17425247.2020.1702644. Issue 1.

[4] T. Waghule, S. Gorantla, V.K. Rapalli, P. Shah, S.K. Dubey, R.N. Saha, G. Singhvi, Emerging trends in topical delivery of curcumin through lipid nanocarriers: effectiveness in skin disorders, AAPS PharmSciTech 21 (7) (2020), https://doi.org/10.1208/s12249-020-01831-9.

[5] A. Singh, C. Shekhar, V.K. Singh, K.R.C. Reddy, Turmeric (Curcuma Longa) an adaptable drug in ayurveda: a review, Indian J. Agric. Allied Sci. 3 (1) (2017) 78–84.

[6] A.R. Vaughn, A. Branum, R.K. Sivamani, Effects of turmeric (Curcuma longa) on skin health: a systematic review of the clinical evidence, Phytother. Res. 2015 (October) (2016) 1243–1264, https://doi.org/10.1002/ptr.5640.

[7] T. Farooqui, A.A. Farooqui, Curcumin: historical background, chemistry, pharmacological action, and potential therapeutic value. Curcumin for Neurological and Psychiatric Disorders: Neurochemical and Pharmacological Properties, Elsevier Inc, 2019, https://doi.org/10.1016/B978-0-12-815461-8.00002-5.

[8] S. Prasad, B. Aggarwal, Turmeric, the golden spice: from traditional medicine to modern medicine, in: I. Benzie, S. Wachtel-Galo (Eds.), Herbal Medicine: Biomolecular and Clinical Aspects, 2nd edition, CRC Press/Taylor & Francis, Boca Raton (FL), 2011. Chapter 13, https://www.ncbi.nlm.nih.gov/books/NBK92752/).

[9] P.M. Reddi, A touch of turmeric: examining an ayurvedic treasure, Adv. Anthropol. 03 (02) (2013) 91–95, https://doi.org/10.4236/aa.2013.32012.

[10] B.E. Bachmeier, D. Melchart, Therapeutic effects of curcumin—from traditional past to present and future clinical applications, Int. J. Mol. Sci. 20 (15) (2019) 3–7, https://doi.org/10.3390/ijms20153757.

[11] A.W.K. Yeung, M. Horbańczuk, N.T. Tzvetkov, A. Mocan, S. Carradori, F. Maggi, J. Marchewka, S. Sut, S. Dall'Acqua, R.Y. Gan, L.P. Tancheva, T. Polgar, I. Berindan-Neagoe, V. Pirgozliev, K. Šmejkal, A.G. Atanasov, Curcumin: total-scale analysis of the scientific literature, Molecules (Basel, Switzerland) 24 (7) (2019), https://doi.org/10.3390/molecules24071393.

[12] Z. Rafiee, M. Nejatian, M. Daeihamed, S.M. Jafari, Application of curcumin-loaded nanocarriers for food, drug and cosmetic purposes, Trends Food Sci. Technol. 88 (April) (2019) 445–458, https://doi.org/10.1016/j.tifs.2019.04.017.

[13] Y. Panahi, O. Fazlolahzadeh, S.L. Atkin, M. Majeed, A.E. Butler, T.P. Johnston, A. Sahebkar, Evidence of curcumin and curcumin analogue effects in skin diseases: A narrative review, J. Cell. Physiol. 234 (2) (2019) 1165–1178, https://doi.org/10.1002/jcp.27096.

[14] S. Gupta, S. Patchva, B. Aggarwal, Discovery of curcumin, a component of the golden spice, and its miraculous biological activities, Clin. Exp. Pharmacol. Physiol. 39 (3) (2012) 283–299, https://doi.org/10.1111/j.1440-1681.2011.05648.x.

[15] S. Gagliardi, C. Morasso, P. Stivaktakis, C. Pandini, V. Tinelli, A. Tsatsakis, D. Prosperi, M. Hickey, F. Corsi, C. Cereda, Curcumin formulations and trials: what's new in neurological diseases, Molecules 25 (22) (2020) 5389, https://doi.org/10.3390/molecules25225389.

[16] M. Hashemzaei, K. Tabrizian, Z. Alizadeh, S. Pasandideh, R. Rezaee, C. Mamoulakis, A. Tsatsakis, Z. Skaperda, D. Kouretas, J. Shahraki, Resveratrol, curcumin and gallic acid attenuate glyoxal-induced damage to rat renal cells, Toxicol. Rep. 7 (2020) 1571–1577, https://doi.org/10.1016/j.toxrep.2020.11.008.

[17] F. Stancioiu, G.Z. Papadakis, S. Kteniadakis, B.N. Izotov, M.D. Coleman, D. A. Spandidos, A. Tsatsakis, A dissection of SARS-CoV2 with clinical implications (Review), Int. J. Mol. Med. 46 (2) (2020) 489–508, https://doi.org/10.3892/ijmm.2020.4636.

[18] B. Salehi, Z. Stojanović-Radić, J. Matejić, M. Sharifi-Rad, N.V. Anil Kumar, N. Martins, J. Sharifi-Rad, The therapeutic potential of curcumin: a review of clinical trials, Eur. J. Med. Chem. 163 (2019) 527–545, https://doi.org/10.1016/j.ejmech.2018.12.016.

[19] W. Guo, Y. Song, W. Song, Y. Liu, Z. Liu, D. Zhang, Z. Tang, O. Bai, Co-delivery of doxorubicin and curcumin with polypeptide nanocarrier for synergistic lymphoma therapy, Sci. Rep. 10 (1) (2020) 1–16, https://doi.org/10.1038/s41598-020-64828-1.

[20] M.M. Yallapu, P.K.B. Nagesh, M. Jaggi, S.C. Chauhan, Therapeutic applications of curcumin nanoformulations, AAPS J. 17 (6) (2015) 1341–1356, https://doi.org/10.1208/s12248-015-9811-z.

[21] S.A. Yousef, Y.H. Mohammed, S. Namjoshi, J.E. Grice, H.A.E. Benson, W. Sakran, M.S. Roberts, Mechanistic evaluation of enhanced curcumin delivery through human skin in vitro from optimised nanoemulsion formulations fabricated with different penetration enhancers, Pharmaceutics 11 (12) (2019), https://doi.org/10.3390/pharmaceutics11120639.

[22] A.L. Luss, P.P. Kulikov, S.B. Romme, C.L. Andersen, C.P. Pennisi, A.O. Docea, A. N. Kuskov, K. Velonia, Y.O. Mezhuev, M.I. Shtilman, A.M. Tsatsakis, L. Gurevich, Nanosized carriers based on amphiphilic poly-N-vinyl-2-pyrrolidone for intranuclear drug delivery, Nanomedicine 13 (7) (2018) 703–715, https://doi.org/10.2217/nnm-2017-0311.

[23] V. Soleimani, A. Sahebkar, H. Hosseinzadeh, Turmeric (Curcuma longa) and its major constituent (curcumin) as nontoxic and safe substances: review, Phytother. Res. 32 (6) (2018) 985–995, https://doi.org/10.1002/ptr.6054.

[24] C.H. Loo, M. Basri, R. Ismail, H.L.N. Lau, B.A. Tejo, M.S. Kanthimathi, H.A. Hassan, Y.M. Choo, Effect of compositions in nanostructured lipid carriers (NLC) on skin hydration and occlusion, Int. J. Nanomedicine 8 (June 2014) (2013) 13–22, https://doi.org/10.2147/IJN.S35648.

[25] S. Sarhadi, M. Gholizadeh, T. Moghadasian, S. Golmohammadzadeh, Moisturizing effects of solid lipid nanoparticles (SLN) and nanostructured lipid carriers (NLC) using deionized and magnetized water by in vivo and in vitro methods, Iran. J. Basic Med. Sci. 23 (3) (2020) 337–343, https://doi.org/10.22038/IJBMS.2020.39587.9397.

[26] V.K. Rapalli, V. Kaul, T. Waghule, S. Gorantla, S. Sharma, A. Roy, S.K. Dubey, G. Singhvi, Curcumin loaded nanostructured lipid carriers for enhanced skin retained topical delivery: optimization, scale-up, in-vitro characterization and assessment of ex-vivo skin deposition, Eur. J. Pharm. Sci. 152 (June) (2020) 105438, https://doi.org/10.1016/j.ejps.2020.105438.

[27] R. López-García, A. Ganem-Rondero, Solid lipid nanoparticles (SLN) and nanostructured lipid carriers (NLC): occlusive effect and penetration enhancement ability, J. Cosmet. Dermatol. Sci. Appl. 05 (02) (2015) 62–72, https://doi.org/10.4236/jcdsa.2015.52008.

[28] S. Shrotriya, N. Ranpise, P. Satpute, B. Vidhate, Skin targeting of curcumin solid lipid nanoparticles-engrossed topical gel for the treatment of pigmentation and irritant contact dermatitis, Artif. Cells Nanomed. Biotechnol. 46 (7) (2018) 1471–1482, https://doi.org/10.1080/21691401.2017.1373659.

[29] S. Hatziantoniou, G. Deli, Y. Nikas, C. Demetzos, G.T. Papaioannou, Scanning electron microscopy study on nanoemulsions and solid lipid nanoparticles containing high amounts of ceramides, Micron 38 (8) (2007) 819–823, https://doi.org/10.1016/j.micron.2007.06.010.
[30] P.S. Kumar, S. Kumar, P. Senthil Kumar, N. Punniamurthy, The Pharma Innovation Journal 2017; 6(4): 07-11 Formulation development and characterization of curcumin loaded solid lipid nanoparticles for improved aqueous solubility and bioavailability, Pharma Innov. J. 6 (4) (2017) 7–11. www.thepharmajournal.com.
[31] V. Dyatlov, T. Seregina, A. Luss, V. Zaitsev, A. Artyukhov, M. Shtilman, A. Chumakova, K. Kushnerev, A. Tsatsakis, Y. Mezhuev, Immobilization of amikacin on dextran: biocomposite materials that release an antibiotic in the presence of bacterial dextranase, Polym. Int. (2020) 0–3, https://doi.org/10.1002/pi.6171.
[32] D.S. Aniesrani Delfiya, K. Thangavel, Evaluation of in vitro release pattern of curcumin loaded egg albumin nanoparticles prepared using acetone as desolvation agent, Curr. Trends Biotechnol. Pharm. 10 (2) (2016) 126–135.
[33] R. Gouda, H. Baishya, Z. Qing, Application of mathematical models in drug release kinetics of carbidopa and levodopa ER tablets, J. Dev. Drugs 06 (02) (2017), https://doi.org/10.4172/2329-6631.1000171.
[34] H.A. Merchant, H.M. Shoaib, J. Tazeen, R.I. Yousuf, Once-daily tablet formulation and in vitro release evaluation of cefpodoxime using hydroxypropyl methylcellulose: a technical note, AAPS PharmSciTech 7 (3) (2006), https://doi.org/10.1208/pt070378.
[35] A. Rezaei, A. Nasirpour, Evaluation of release kinetics and mechanisms of curcumin and curcumin-β-cyclodextrin inclusion complex incorporated in electrospun almond gum/PVA nanofibers in simulated saliva and simulated gastrointestinal conditions, BioNanoScience 9 (2) (2019) 438–445, https://doi.org/10.1007/s12668-019-00620-4.
[36] T. Gupta, J. Singh, S. Kaur, S. Sandhu, G. Singh, I.P. Kaur, Enhancing bioavailability and stability of curcumin using solid lipid nanoparticles (CLEN): a covenant for its effectiveness, Front. Bioeng. Biotechnol. 8 (October) (2020) 1–14, https://doi.org/10.3389/fbioe.2020.00879.
[37] A. Kryczyk-Poprawa, A. Kwiecień, W. Opoka, Photostability of topical agents applied to the skin: a review, Pharmaceutics 12 (1) (2020), https://doi.org/10.3390/pharmaceutics12010010.
[38] M.R. Patel, R.B. Patel, J.R. Parikh, B.G. Patel, Improving the isotretinoin photostability by incorporating in microemulsion matrix, ISRN Pharm. 2011 (2011) 1–6, https://doi.org/10.5402/2011/838016.
[39] D. Demirovic, S.I.S. Rattan, Curcumin induces stress response and hormetically modulates wound healing ability of human skin fibroblasts undergoing ageing in vitro, Biogerontology 12 (5) (2011) 437–444, https://doi.org/10.1007/s10522-011-9326-7.
[40] A. Suarez-Arnedo, F.T. Figueroa, C. Clavijo, P. Arbeláez, J.C. Cruz, C. Muñoz-Camargo, An image J plugin for the high throughput image analysis of in vitro scratch wound healing assays, PLoS One 15 (7 July) (2020) 1–14, https://doi.org/10.1371/journal.pone.0232565.
[41] J. Yoo, Y.Y. Won, Phenomenology of the initial burst release of drugs from PLGA microparticles, ACS Biomater. Sci. Eng. 6 (11) (2020) 6053–6062, https://doi.org/10.1021/acsbiomaterials.0c01228.
[42] I.Y. Wu, S. Bala, N. Škalko-basnet, M. Pio di Cargo, Interpreting non-linear drug diffusion data : Utilizing Korsmeyer-Peppas model to study drug release from liposomes, Eur. J. Pharm. Sci. 138 (July) (2019) 105026, https://doi.org/10.1016/j.ejps.2019.105026.
[43] M.A. Rahman, N. Ahmed, I. Hasan, M.S. Reza, Formulation and in vitro assessment of Eudragit L 100 and Eudragit S 100 based naproxen microspheres, Dhaka Univ. J. Pharm. Sci. 15 (1) (2016) 47–55, https://doi.org/10.3329/dujps.v15i1.29192.
[44] H.N.M. Saari, L.S. Chua, R. Hasham, L. Yuliati, Curcumin-loaded nanoemulsion for better cellular permeation, Sci. Pharm. 88 (4) (2020) 1–12, https://doi.org/10.3390/scipharm88040044.
[45] H. Lee, M. Jeong, Y. Na, S. Kim, H. Lee, C. Cho, An EGF- and curcumin-co-encapsulated nanostructured lipid carrier accelerates chronic-wound healing in diabetic rats, Molecules 25 (2020) 4610, https://doi.org/10.3390/molecules25204610.
[46] C. Righeschi, M.C. Bergonzi, B. Isacchi, C. Bazzicalupi, P. Gratteri, A.R. Bilia, Enhanced curcumin permeability by SLN formulation: the PAMPA approach, Lwt – Food Sci. Technol. 66 (2016) 475–483, https://doi.org/10.1016/j.lwt.2015.11.008.
[47] N. Ahmad, R. Ahmad, A. Al-Qudaihi, S.E. Alaseel, I.Z. Fita, M.S. Khalid, F. H. Pottoo, Preparation of a novel curcumin nanoemulsion by ultrasonication and its comparative effects in wound healing and the treatment of inflammation, RSC Adv. 9 (35) (2019) 20192–20206, https://doi.org/10.1039/c9ra03102b.
[48] R.S. Nair, A. Morris, N. Billa, C.O. Leong, An evaluation of curcumin-encapsulated chitosan nanoparticles for transdermal delivery, AAPS PharmSciTech 20 (2) (2019) 1–13, https://doi.org/10.1208/s12249-018-1279-6.
[49] I. Vrouvaki, E. Koutra, M. Kornaros, K. Avgoustakis, F.N. Lamari, S. Hatziantoniou, Polymeric nanoparticles of Pistacia lentiscus var. Chia essential oil for cutaneous applications, Pharmaceutics 12 (4) (2020), https://doi.org/10.3390/pharmaceutics12040353.
[50] P. Iriventi, N.V. Cupta, Topical delivery of curcumin and caffeine mixture-loaded nanostructured lipid carriers for effective treatment of psoriasisle, Pharmacogn. Mag. 16 (68) (2020) 206–217, https://doi.org/10.4103/pm.pm_260_19.
[51] D.S. Coelho, V.E.B. de Campos, Z.M.F. Freitas, E. Ricci Júnior, M.B. Caarls, B. Lourenço Diaz, E.P. dos Santos, M.S. Mariana, Development and characterization of nanoemulsion containing almond oil, biodegradable polymer and propranolol as potential treatment in Hemangioma, Macromol. Symp. 381 (1) (2018) 1–11, https://doi.org/10.1002/masy.201800121.
[52] L. Montenegro, C. Parenti, R. Turnaturi, L. Pasquinucci, Resveratrol-loaded lipid nanocarriers: correlation between in vitro occlusion factor and in vivo skin hydrating effect, Pharmaceutics 9 (4) (2017), https://doi.org/10.3390/pharmaceutics9040058.
[53] H. Hamishehkar, S. Same, K. Adibkia, K. Zarza, J. Shokri, M. Taghaee, Maryam Kouhsoltani, A comparative histological study on the skin occlusion performance of a cream made of solid lipid nanoparticles and Vaselinee, Res. Pharm. Sci. 10 (5) (2015) 378–387.
[54] K. Gardikis, S. Hatziantoniou, K. Viras, C. Demetzos, Effect of a bioactive curcumin derivative on DPPC membrane: a DSC and Raman spectroscopy study, Thermochim. Acta 447 (1) (2006) 1–4, https://doi.org/10.1016/j.tca.2006.03.007.
[55] E. Alkhader, C.J. Roberts, R. Rosli, K.H. Yuen, E.K. Seow, Y.Z. Lee, N. Billa, Pharmacokinetic and anti-colon cancer properties of curcumin-containing chitosan-pectinate composite nanoparticles, J. Biomater. Sci. Polym. Ed. 29 (18) (2018) 2281–2298, https://doi.org/10.1080/09205063.2018.1541500.
[56] N. Golda, J. Koo, H.I. Maibach, Effects and uses of occlusion on human skin: an overview, Cutan. Ocul. Toxicol. 24 (2) (2005) 91–104, https://doi.org/10.1081/CUS-200059571.
[57] K. Kobaly, A.K. Somani, T. McCormick, S.T. Nedorost, Effects of occlusion on the skin of atopic dermatitis patients, Dermatitis 21 (5) (2010) 255–261, https://doi.org/10.2310/6620.2010.10013.
[58] H. Zhai, H.I. Maibach, Skin occlusion and irritant and allergic contact dermatitis: an overview, Contact Derm. 44 (4) (2001) 201–206, https://doi.org/10.1034/j.1600-0536.2001.044004201.x.
[59] https://www.clinicaltrials.gov, accessed in January 2021.